PCCP

PAPER

View Article Online
View Journal | View Issue

Cite this: *Phys. Chem. Chem. Phys.*, 2025, **27**, 24620

κ-Casein inhibits amorphous aggregation of β-casein

Jaspreet Kaur and Mily Bhattacharya *

Received 25th June 2025,
Accepted 17th October 2025

DOI: 10.1039/d5cp02431e

rsc.li/pccp

Caseins are mammalian milk proteins that are commonly utilized in food industries due to their various nutritional and functional properties. Among various caseins, *viz.* α_{S1}-, α_{S2}-, β- and κ-casein, β-casein acts as a natural emulsifier and foam stabilizer as well as a molecular chaperone. However, these properties get significantly altered during food processing, which raises concerns about the food quality. Recently, there has been an increasing interest in using chaperone-like molecules to restrict the aggregation of food proteins. Here we show that κ-casein, which coexists with β-casein in milk micelles, exhibits its chaperonic activity and can effectively inhibit calcium ion-induced amorphous aggregation of β-casein in a dose-dependent manner. Using turbidity assays, dynamic light scattering, and electron microscopy, we demonstrate that inter-protein complexes comprising β- and κ-caseins are formed that preclude the binding of calcium ions (Ca^{2+}) to β-casein. This further impedes the multivalent interactions between β-casein polypeptides, thus inhibiting inter-casein interactions required for spontaneous Ca^{2+}-induced β-casein self-assembly. We also report the disintegration of pre-formed β-casein aggregates upon the addition of κ-casein, which may have implications in devising strategies for regulating the assembly and disassembly processes of β-casein and other food proteins.

1. Introduction

Protein aggregation ensues upon the spontaneous self-assembly of misfolded/partially-unfolded proteins into ordered fibrillar amyloids and/or disordered amorphous aggregates due to conformational perturbations in the native protein as a consequence of chemical or thermal or oxidative stresses, mutational effects, exposure to toxic agents, unfavorable protein–protein interactions, *etc.*[1–5] Nevertheless, cells employ both intra- and extracellular molecular chaperones that play a significant role in maintaining the cellular protein homeostasis, ensure that proteins fold correctly and also prevent protein misfolding and aggregation.[6–9] The molecular chaperones are mainly classified into two categories, namely, foldase- and holdase chaperones. The foldases are ATP-dependent chaperones that ascertain correct folding of proteins, whereas the holdases are non-ATP-dependent chaperones that inhibit both fibrillar and amorphous aggregation of proteins by forming high molecular weight complexes, stabilizing the partially-folded intermediates, and preventing the undesirable "mis-interactions" within aggregation-competent species.[10,11] The foldases and holdases function together in a synergistic manner to maintain cellular proteostasis and avoid the accrual of any toxic species related to protein aggregation. However, any dysfunction of chaperones leads to aberrant folding of proteins and accumulation of toxic intermediates, resulting in protein aggregation that leads to various pathologies. Although the uncontrolled self-assembly of proteins is implicated in a variety of neurodegenerative disorders and systemic diseases, several studies have indicated the involvement of protein aggregates in the pharmaceutical industry as well as in food processing and food formulation industries.[11–13] While food protein aggregates play beneficial roles during gelation, stabilizing foams and emulsions, they may also lead to undesired alteration of the microstructure of protein-rich foods during food processing and storage, leading to changes in the nutritional, techno-functional, and organoleptic properties.[11,14] Consequently, the digestion and absorption of food proteins are significantly affected.[15,16] Therefore, there is a pressing need to devise and design strategic targeted inhibitors that can impede and/or reverse food protein aggregation.

Caseins are intrinsically disordered proteins (IDPs), found in mammalian milk, which are also known as secreted calcium phosphate-binding phosphoproteins (SCPPs).[17–20] Bovine milk is rich in ~80% caseins that comprise four different casein polypeptides, namely, α_{S1}-, α_{S2}-, β- and κ-casein at molar ratios of 4 : 1 : 4 : 1, respectively, as detected by capillary zone electrophoresis[21] and high-performance liquid chromatography (HPLC).[22] The extracellular caseins exhibit sequence-diversity and "multiple proteoforms"[23] owing to varying extents of post-translational modifications (PTMs) such as *O*-glycosylation in

Department of Chemistry and Biochemistry, Thapar Institute of Engineering and Technology, Patiala-147004, Punjab, India. E-mail: mily.bhattacharya@thapar.edu

κ-casein and phosphorylation in α_{S1}-, α_{S2}-, and β-caseins. The preponderance of proline (P) and glutamine (Q)-rich sequences promote a polyproline-II (PP-II) conformation in caseins, rendering them as hydrophilic IDPs that facilitate binding between the conformationally-dynamic polypeptide chains and calcium phosphate (CaP) nanoclusters, leading to casein micelles. The highly-hydrated micelles are polydisperse and form fuzzy complexes mediated by multivalent inter-casein interactions encompassing short linear sequence motifs (SLiMs) such as CaP-SLiM, basic SLiM, hydrophobic and order promoting-SLiM, and zipper-SLiM.[17–20,24] Moreover, α_{S1}-, α_{S2}-, and β-caseins are known to be calcium-sensitive caseins since they can be precipitated by lower concentrations of calcium salts. In contrast, κ-casein is known to be a calcium-insensitive casein since it remains soluble in the presence of low calcium salt concentrations and does not form precipitates. Recent studies using a multivalent binding model have shown that the casein micelles adopt a ''coat-core structure,'' wherein the caseins bound to CaP nanoclusters occur in the core, and the free, unbound caseins occur both in the core and the coat.[24] According to the multivalent binding model, κ-casein is present both in the core and the coat of the micelles, in contrast to the traditional hydrophobic colloid model, and almost equal proportions of α_{S1}-, β- and κ-caseins were calculated to be present in the coat of the micelles.[17,18,24] All of these bovine caseins reportedly form cross β-sheet-rich amyloid fibrils under conducive solution conditions and therefore, studies have suggested that amyloid formation is a generic property of the casein polypeptides.[25–30] Caseins exhibit a wide range of applications in food systems as well as in non-food systems, many of which utilize their unique aggregation properties. The aggregation behavior of casein is relevant in various multidisciplinary domains, such as the food, material science and nanotechnology, biomedical and pharmaceutical industries, along with functional food engineering. Elucidating the casein aggregation mechanisms and devising potential preventive strategies to combat casein aggregation may assist materials scientists, biotechnologists, engineers, and industrialists.[17,31–33] However, the caseins also behave as holdase-type, ATP-independent molecular chaperones, similar to intracellular sHsps such as α-crystallin and extracellular clusterin, and exhibit promiscuity by binding to a diverse range of proteins and inhibiting their aggregation.[12,18,19,34] Although the caseins share dynamical and functional similarities with sHsps and clusterin, they do not share any structural similarities with these molecular chaperones. Caseins have been shown to inhibit, with variable efficiencies, the chemical, thermal, and light stress-induced unfolding and prevent amorphous and/or amyloid aggregation of globular proteins such as, DTT-reduced insulin, α-lactalbumin, β-lactoglobulin, insulin, lysozyme, alcohol dehydrogenase, catalase, amyloid β-peptide, *etc.*[12,17,23,26,35–40] Almost all of these studies demonstrated the inhibitory efficacies of α_S- and β-caseins, wherein, the chaperone-like activity was primarily attributed to α_{S1}- and β-caseins due to their preponderance in bovine milk. While it has been suggested that the chaperonic activity of caseins may be primarily attributed to the free caseins (*viz.* α_{S1}-, β- and κ-caseins) present in the micellar coat, that can exchange more quickly between the serum and micelle compared to the CaP-bound caseins present in the core of the micelles,[25] reports on the chaperonic activity of κ-casein appear to be extremely scarce despite its predominance in the micellar coat. Additionally, the amyloid fibrillation propensities of α_{S2}- and κ-caseins were demonstrated to be higher compared to their chaperonic activities,[41] and the fibril formation from these caseins was effectively suppressed by α_{S1}- and β-caseins.[29] It has also been reported that a bi-chaperone system involving both β-casein and α-crystallin suppresses insulin aggregation by exhibiting ''synergistic chaperonic operation'' facilitated *via* electrostatic interactions between the polar-charged domains of the chaperones.[42] However, a few recent reports indicated that the chaperonic β-casein formed amorphous aggregates upon the addition of calcium chloride ($CaCl_2$) under physiological conditions.[43,44] Therefore, in this study, we explored the chaperonic action of κ-casein towards the amorphous aggregation of β-casein triggered by divalent calcium ions using light scattering and microscopic techniques. Additionally, we investigated sodium chloride (NaCl)-induced dissolution of preformed β-casein aggregates that allowed us to gain deeper insights into the plausible inhibitory measures and their mode of chaperonic activity in preventing β-casein aggregation.

2. Results and discussion

2.1. Sodium chloride (NaCl)-induced dissolution of preformed β-casein amorphous aggregates

Recently, we demonstrated that Ca^{2+} ion-induced β-casein aggregation under physiological conditions is governed by binding of the Ca^{2+} ions to a CaP-SLiM in β-casein that facilitates the formation of inter-casein linkages and multivalent interactions mediated by neutral, polar and charged residues, between the β-casein polypeptides.[44] The contribution of hydrophobic interactions during the self-assembly was suggested to be negligible compared to β-casein–$CaCl_2$ interactions. Additionally, we have demonstrated that Ca^{2+} ion-induced β-casein aggregation can be abolished upon the addition of sodium chloride (NaCl; pre-added) due to electrostatic screening of the polypeptides that precludes the binding between calcium ions and the phosphorylated serine residues of the protein and hence, impedes the pivotal step towards protein self-assembly.[44] Next, we asked whether multivalent interactions encompassing neutral, polar, and charged residues between the β-casein polypeptides are indeed critical for the self-assembly. To address this issue, we added 150 mM NaCl (post-addition) to the preformed Ca^{2+}-induced β-casein aggregates and monitored the changes in the turbidity of the aggregates' solution visually (Fig. 1a). We observed that the solution turbidity decreased rapidly upon the addition of 150 mM NaCl and became clear, presumably due to the dissolution of the β-casein aggregates. To verify our proposition, we performed time-dependent dynamic light scattering (DLS) experiments that allowed us to watch the changes in the hydrodynamic diameters (D_h) of the protein samples in a

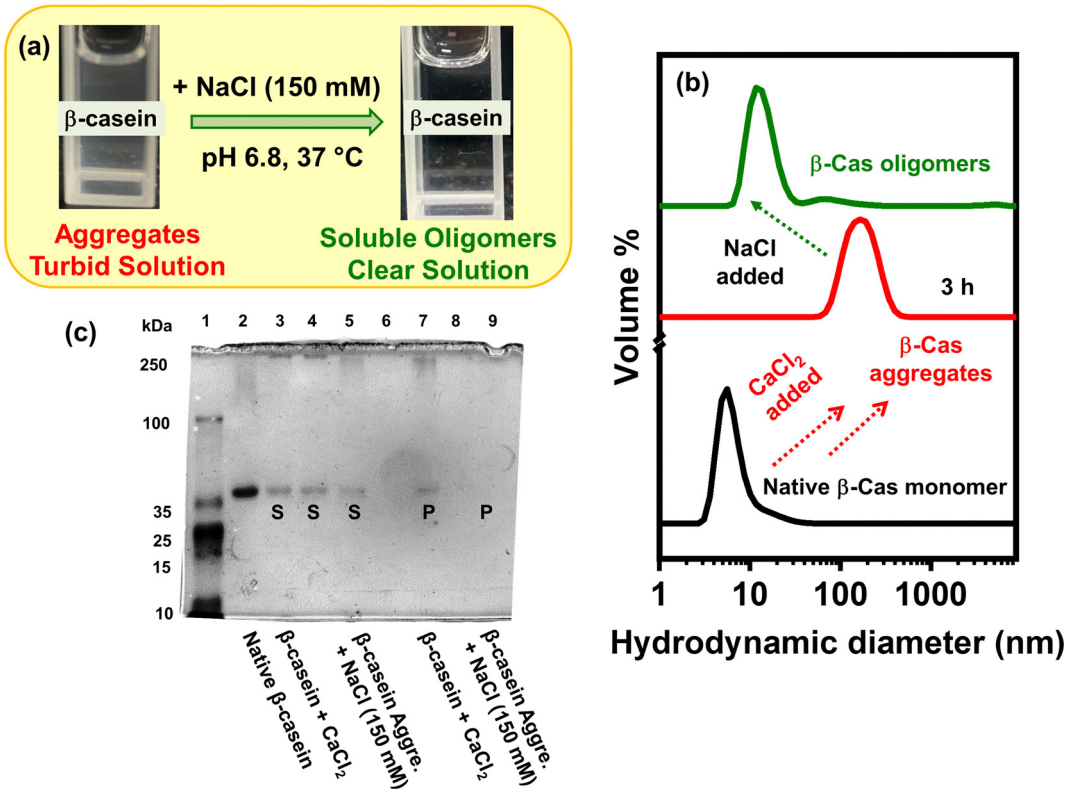

Fig. 1 Disruption of Ca^{2+}-induced β-casein aggregates formed at pH 6.8, 37 °C upon the addition of 150 mM sodium chloride (NaCl) to the preformed aggregates. (a) Disappearance of the solution turbidity, observed visually, resulting in a clear solution. (b) Hydrodynamic diameter of the native β-casein (black) and β-casein aggregates (red) formed after 3 h of incubation in the presence of 2.5 mM $CaCl_2$, pH 6.8, 37 °C, monitored using dynamic light scattering (DLS), depicted by a stack-plot representation. A significant reduction in the hydrodynamic diameter of β-casein aggregates, upon the addition of 150 mM NaCl (shown by a green dashed arrow), indicates dissolution of the aggregates leading to aggregation-incompetent, soluble oligomers (green). (c) Native-PAGE analyses of native β-casein monomer (lane 2), Ca^{2+}-induced β-casein aggregates formed at ~37 °C (lanes 3 and 7) and upon the addition of 150 mM NaCl (post-addition approach) into the preformed β-casein aggregates after 3 h of incubation (lanes 5 and 9) (S: supernatant, P: pellet).

temporal manner. We conjectured that a reduction in the overall hydrodynamic size could be directly correlated to the dissolution of aggregates upon the addition of NaCl. As expected, the monomeric β-casein (D_h: ~7 nm; Fig. 1b) formed large-sized aggregates (~200 nm; Fig. 1b) upon the addition of $CaCl_2$ at pH 6.8, 37 °C which corroborates the previous report.[44] Upon the addition of 150 mM NaCl to the preformed aggregates, we observed an immediate decrease in the hydrodynamic diameter from ~200 nm to ~12 nm, suggesting a rapid disruption of β-casein aggregates to smaller, soluble oligomers (Fig. 1b) resulting in a clear solution. We also performed native-PAGE experiments (Fig. 1c) to examine the disaggregation of preformed Ca^{2+}-induced β-casein aggregates upon the addition of 150 mM NaCl. Analyses of the β-casein aggregates' samples revealed that both the supernatant and the pellet largely comprised β-casein monomers and high molecular weight aggregates, respectively. Upon the addition of NaCl to the pre-formed aggregates, we observed β-casein monomer bands primarily in the supernatant (Fig. 1c). We could not detect any high molecular weight protein aggregates in the pellet, which reaffirmed NaCl-induced disruption of the β-casein amorphous aggregates. The results are in accordance with the turbidity assay (Fig. 1a) and the DLS measurements (Fig. 1b). Therefore, based on these findings, we inferred that the addition of NaCl disrupted the multivalent interactions between the intrinsically disordered β-casein chains due to electrostatic screening of the charged residues in β-casein. This electrostatic shielding probably induced charge redistribution, which further diminished the possibility of inter-casein interactions.[45,46] Therefore, it was evident that multivalent interactions encompassing neutral, polar, and charged residues between the β-casein polypeptides are indeed essential for Ca^{2+} ion-induced β-casein self-association. Recently, it has been shown that NaCl can disrupt globular protein-based amorphous aggregates, which leads to an apparent refolding of the protein to its native state.[47] However, to the best of our knowledge, such an observation on the salt-induced disintegration of preformed IDP-based aggregates, is reported here for the first time, and it may offer a novel way to control the self-assembly and disassembly of β-casein.

2.2. Conformational characteristics and charge patterning of β- and κ-caseins

In the casein micelles, since β-casein coexists with other caseins, *viz.* α_{S1}-, α_{S2}-, and κ-caseins that act as molecular chaperones for each other, we next set out to examine whether

κ-casein exhibits chaperonic activity towards the Ca^{2+} ion-induced self-assembly of intrinsically-disordered β-casein (Fig. 2a) that leads to amorphous aggregates under physiological conditions. κ-Casein comprises 169 amino acid residues (Fig. 2b) wherein the preponderance of prolines (P) and glutamines (Q) renders the protein to be intrinsically disordered, as evident from its far UV-CD spectrum (Fig. 2b and 3a),[48] that is similar to β-casein (Fig. 2a and 3a). Analyses of the charge distribution on both β- and κ-caseins, using the classification of intrinsically disordered ensemble relationships (CIDER) algorithm,[49,50] revealed that β-casein comprises clusters of positively- and negatively-charged residues, coexisting at specific positions, along the polypeptide chain with a predominance of negative charges at the N-terminus (Fig. 3b) as was also reported earlier.[44] On the other hand, κ-casein exhibited charged residues distributed almost uniformly along the entire chain length. However, the negatively-charged residues were mostly populated at the C-terminus, whereas the positively-charged residues were located at the N-terminus and mostly in the middle of the polypeptide chain (Fig. 3c). Therefore, based on the charge patterning of both β- and κ-caseins, we hypothesized that these proteins can interact electrostatically whereby, the positively-charged residues of κ-casein may induce charge compensation at the N-terminus of β-casein. Consequently, the binding of Ca^{2+} ions to β-casein (*via* CaP-SLiM) will be impeded, leading to the inhibition of Ca^{2+}-induced protein amorphous assembly.

2.3. Monomerization of κ-casein for investigating its chaperonic activity in inhibiting Ca^{2+}-induced β-casein amorphous assembly

Prior to validating our hypothesis, we monomerized κ-casein to decipher the inter-protein interactions between β- and κ-caseins at the molecular level. Since κ-casein rapidly forms micelles mediated *via* intermolecular disulfide bonds owing to the two cysteine residues present within the protein, we chemically modified the cysteines using a well-known protocol[41,51] that yielded reduced- and carboxymethylated (RCM) κ-casein (for details, please see the SI). Such chemical modification is expected to result in predominantly monomeric κ-casein (*i.e.* RCM κ-casein), irrespective of its concentration and throughout the timescale of our experiments, during its interactions with the monomeric β-casein (10 μM used in this study). Moreover, to study the chaperonic activity of RCM κ-casein towards Ca^{2+}-induced β-casein amorphous aggregation, we implemented a two-pronged methodology, namely, pre-addition and post-addition of RCM κ-casein (for details, please see the SI) as described in the following sections.

2.4. Probing into the chaperonic activity of monomeric κ-casein (pre-added) by turbidity assays

Herein, we describe the results obtained from the turbidity assays that serve as quick indicators of protein aggregation. At first, we examined the changes in the solution turbidity visually. For our pre-addition-based experiments (for details, please see the SI), we added monomeric RCM κ-casein into pH 6.8, imidazole-HCl buffer followed by 2.5 mM $CaCl_2$ and β-casein at room temperature (~25 °C) and the reaction mixture was incubated at 37 °C. Previous reports[43,44] have indicated that β-casein formed large-sized, amorphous aggregates, upon the addition of $CaCl_2$ at pH 6.8, 37 °C, resulting in a turbid solution. Therefore, as expected, we also obtained similar results in the absence of κ-casein (Fig. 3d). However, in the presence of monomeric κ-casein, we found that the β-casein solution

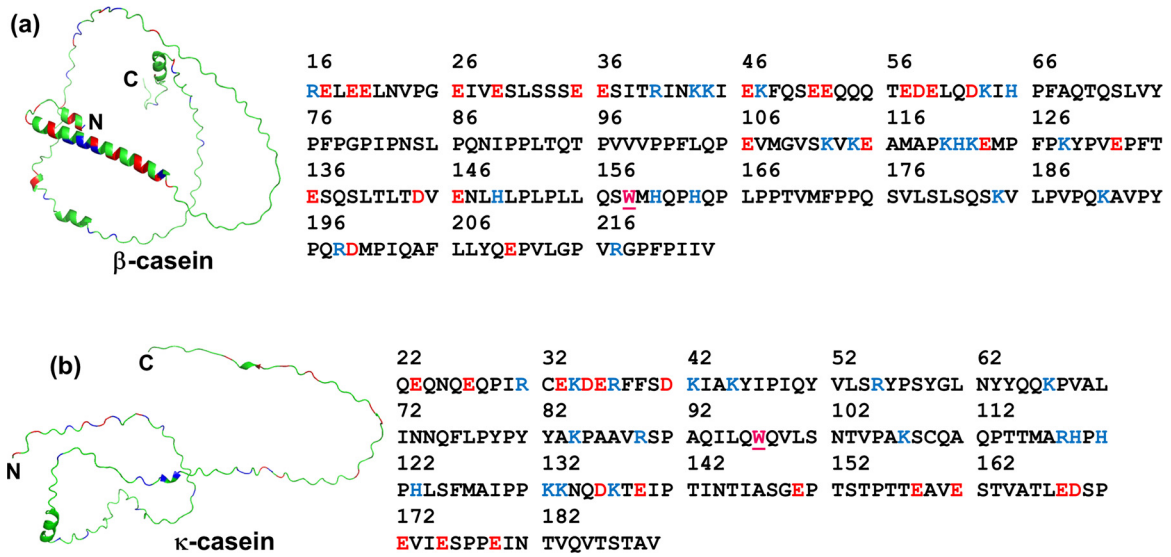

Fig. 2 (a) Structure of β-casein (UniProt ID: P02666; signal peptide deleted) predicted by AlphaFold (average pLDDT score: 61 wherein, pLDDT implies confidence of prediction) along with the amino acid sequence of β-casein. (b) Structure of κ-casein (UniProt ID: P02668; signal peptide removed) predicted by AlphaFold (average pLDDT score: 54) accompanied by its amino acid sequence. A pLDDT score between 50–70 is generally obtained for conformationally-dynamic intrinsically disordered proteins (IDPs), resulting in a low prediction accuracy. The positively- and negatively-charged amino acid residues in both the structures and the sequences are represented in blue and red, respectively, and tryptophan residues are shown in pink (underlined).

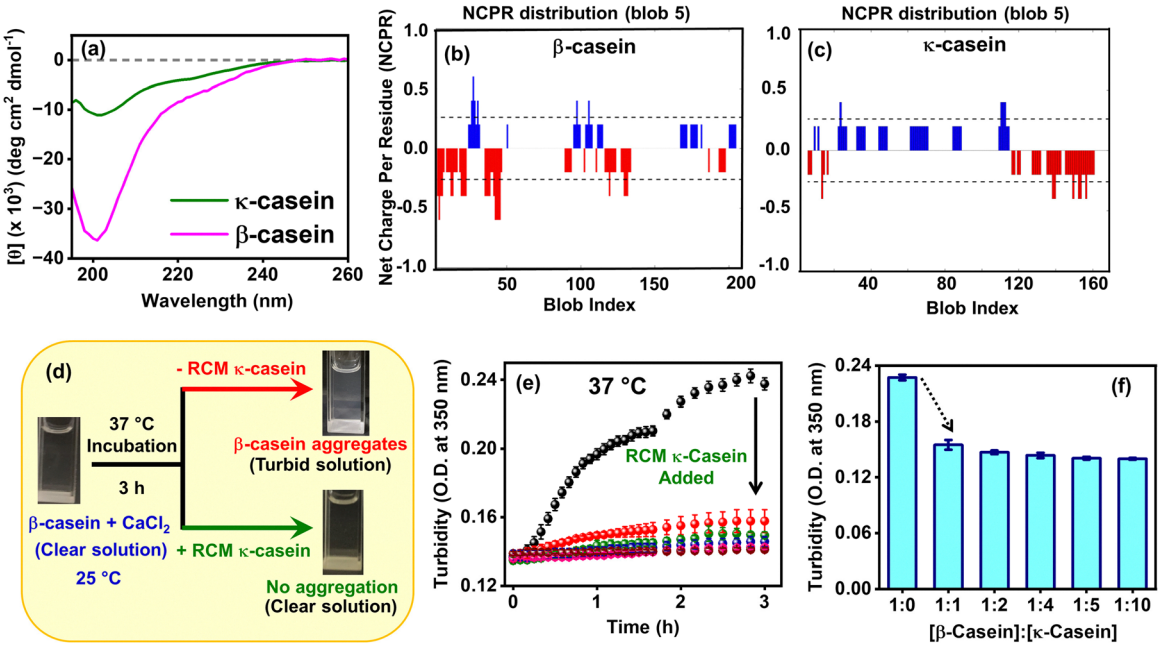

Fig. 3 (a) Far UV-CD spectra of reduced and carboxymethylated (RCM) native κ-casein and β-casein monomers. (b) and (c) The net charge per residue (NCPR) analyses, depicting the charge distribution profiles of (b) β-casein and (c) κ-casein. Fig. 3b was reprinted from our previous publication (ref. 44), Copyright (2025), with permission from Elsevier. (d) Schematic representation of the changes in β-casein solution turbidity upon the addition of $CaCl_2$, monitored visually, in the absence and in the presence of RCM κ-casein at 37 °C. The cuvettes depicted here for the clear solution are the same. (e) Monitoring quantitative changes in the solution turbidity (optical density (O.D) measured at 350 nm) of Ca^{2+}-induced β-casein (10 μM) aggregation at 37 °C in the absence (black) and in the presence of variable concentrations of RCM κ-casein (pre-addition), *viz.*, 10 μM (red), 20 μM (olive), 40 μM (blue), 50 μM (pink), and 100 μM (brown). (f) Bar-plot representation of the decrease (black dashed arrow) in the solution turbidity, collected after 2 h, in the absence and in the presence of RCM κ-casein in a dose-dependent manner.

remained clear at 37 °C (Fig. 3d) even for prolonged hours (≥3 h) of incubation in the presence of $CaCl_2$. This suggested a plausible hindrance to the binding of calcium ions to β-casein, mediated by κ-casein monomers due to inter-casein electrostatic interactions, leading to an inhibition of Ca^{2+}-induced amorphous assembly of β-casein.

To gain further insights into the presumed chaperonic activity of κ-casein in inhibiting β-casein aggregation, we next determined the changes in the solution turbidity quantitatively (optical density measurements at 350 nm) of the reaction mixture at 37 °C in the presence of variable concentrations of RCM κ-casein (pre-addition-based experiments; Fig. 3e).[52] Such concentration-dependent experiments allowed us to ascertain the optimum concentration of monomeric κ-casein required for exhibiting its chaperone-like activity. The molar ratios of β-casein : RCM κ-casein were chosen as 1 : 1, 1 : 2, 1 : 4, 1 : 5, and 1 : 10, wherein the concentration of β-casein was fixed at 10 μM and that of κ-casein monomer was varied (10–100 μM). In the absence of κ-casein, the solution turbidity at 37 °C was quite high owing to the formation of Ca^{2+} ion-induced β-casein aggregates. In the presence of monomeric κ-casein, the turbidity reduced substantially (∼30% at 1 : 1 molar ratio) and thereafter, progressively (up to ∼40%; at ≥1 : 5 molar ratio) as a function of increasing concentration of κ-casein (Fig. 3e and f). Therefore, the results from the turbidity assays suggested that (i) the ≥1 : 4 molar ratio of monomeric κ-casein was optimal for its chaperonic activity, and (ii) electrostatic shielding of the β-casein polypeptide by κ-casein, mediated *via* polar, oppositely-charged residues, prevented Ca^{2+} ions from binding to the phosphorylated serines (CaP-SLiM) of β-casein. Moreover, an overall reduction in the solution turbidity, upon the pre-addition of RCM κ-casein, indicated a decrease in the extent of β-casein aggregation and presumably, a reduction in the size of the aggregates. This could be attributed to the formation of a fuzzy coat by the C-terminal region of κ-casein, which acted as a steric and an electrostatic barrier.[53] Consequently, the amorphous aggregation of β-casein, triggered by calcium ions, was significantly diminished. We next directed our efforts to directly witness the inhibitory action of monomeric κ-casein on β-casein aggregation as described in the following section.

2.5. Examining the chaperonic activity of monomeric κ-casein (pre-added) by DLS measurements and TEM imaging

To examine the chaperone-like activity of monomeric κ-casein in preventing Ca^{2+}-induced β-casein aggregation, we monitored temporal changes in the overall size of the protein sample as well as the nanoscopic morphologies using the dynamic light scattering (DLS) technique in conjunction with TEM imaging (Fig. 4a–g). These experiments enabled us to directly witness the changes in the hydrodynamic diameters (Fig. 4b, d and f) and the morphological characteristics (Fig. 4a, c, e and g) of the aggregation reaction mixture of β-casein, in the absence (Fig. 4a) and in the presence (Fig. 4c, e and g) of κ-casein monomers, in a time-dependent and dose-dependent (κ-casein) manner. Prior

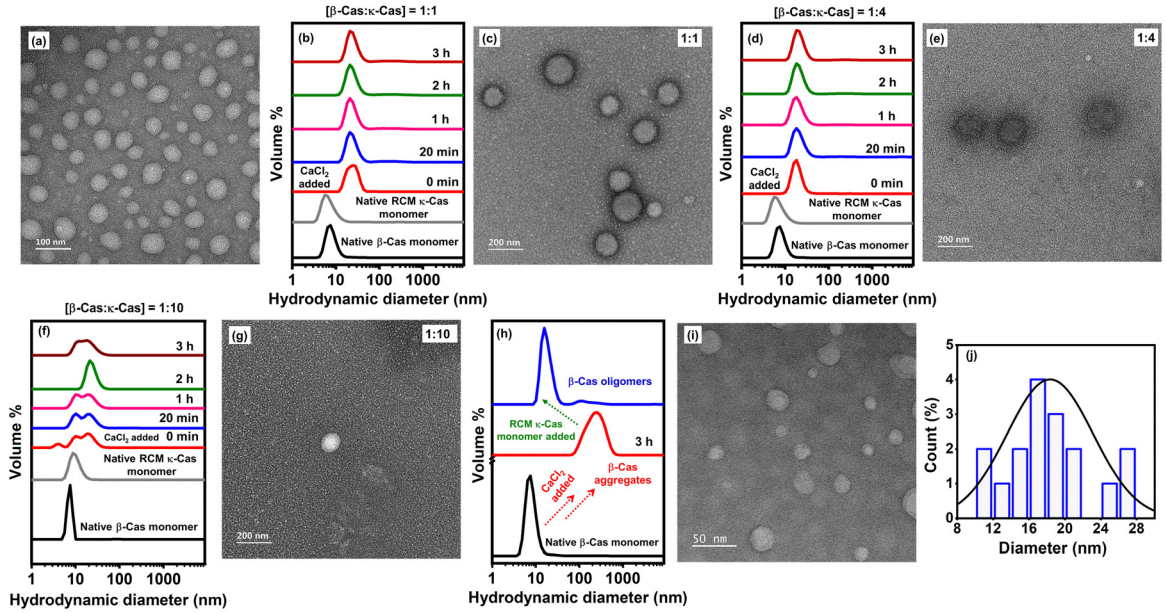

Fig. 4 (a) Morphology of the Ca^{2+}-induced β-casein aggregates, formed at 37 °C in the absence of reduced and carboxymethylated (RCM) κ-casein, obtained using transmission electron microscopy (TEM). Scale bar: 100 nm. (b)–(g) Alterations in the hydrodynamic diameters (b), (d) and (f), measured by dynamic light scattering (DLS), and nanoscopic morphologies (c), (e) and (g), obtained using transmission electron microscopy (TEM), of $CaCl_2$-induced β-casein aggregates/oligomers formed, at 37 °C, in the presence of RCM κ-casein (pre-addition) at varied molar ratios of β-casein:κ-casein, *viz.*, (b) and (c) 1 : 1 (*i.e.*, 10 μM of β- and κ-casein each), (d) and (e) 1 : 4 (*i.e.*, 10 μM of β- and 40 μM of RCM κ-casein), and (f) and (g) 1 : 10 (*i.e.*, 10 μM of β- and 100 μM of RCM κ-casein). In all of the hydrodynamic diameter-based stack-plot representations, native β-casein monomer is depicted by a black line and the same light scattering data of the native β-casein have been plotted in all of the DLS data (b), (d) and (f) shown here. In all of the TEM images (c), (e) and (g), scale bar: 200 nm. (h) Hydrodynamic diameter of the native β-casein (black) and β-casein aggregates (red) formed after 3 h of incubation. Disintegration of the preformed β-casein amorphous aggregates (shown by green dashed arrow) into oligomers (blue) upon the addition of 40 μM RCM κ-casein (post-addition). (i) TEM image of the β-casein sample following the post-addition of RCM κ-casein and (j) its respective histogram depicting the size-distribution of the disintegrated β-casein aggregates. Scale bar: 50 nm.

to setting up the aggregation reactions, we measured the hydrodynamic diameters of both monomeric RCM κ-casein (at various concentrations, *viz.* 10, 40, and 100 μM) and β-casein (10 μM) separately. RCM κ-casein showed a hydrodynamic diameter (D_h) of ~7–10 nm (Fig. 4b, d, f and Fig. S1a, b), indicating that it indeed remained monomeric irrespective of its concentration. However, during several repetitions of the same experiments, we did observe RCM κ-casein oligomers (D_h: ~15 nm) at 100 μM protein concentration (Fig. S1a and c). This could be attributed to the propensity of RCM κ-casein to undergo oligomerization at 37 °C. On the other hand, monomeric β-casein showed a hydrodynamic diameter of ~7 nm (Fig. 4b, d and f) as expected, and both of these values were in accordance with the previous reports.[44,54,55] Upon initiating the aggregation by adding 2.5 mM $CaCl_2$ at pH 6.8, 37 °C to β-casein solution, we observed that β-casein formed larger aggregates (~200 nm; Fig. 1b and 4a), in the absence of κ-casein monomers, as reported earlier.[44] However, in the presence of pre-added RCM κ-casein at varied molar ratios (*viz.* 1 : 1, 1 : 4, and 1 : 10), we observed the following (Fig. 4b, d and f): (i) the formation of soluble, aggregation-incompetent oligomers whose average hydrodynamic sizes were ~22 nm (Fig. 4b), ~18 nm (Fig. 4d), and a bimodal distribution of both ~10 and ~18 nm (Fig. 4f and Fig. S1d) at β-casein : κ-casein molar ratios of 1 : 1, 1 : 4, and 1 : 10, respectively, and (ii) the absence of any large-sized (≥100 nm) β-casein aggregates in the reaction mixture. These findings suggested that the pre-added κ-casein monomers suppressed Ca^{2+} ion-induced β-casein aggregation completely and led to the formation of largely β-casein oligomers. However, the possibility of the formation of a β-casein–κ-casein inter-protein complex, due to an effective shielding of the β-casein polypeptide chain by the κ-casein monomers, cannot be ruled out that can further inhibit the binding of calcium ions to β-casein CaP-SLiMs, hence, inhibiting β-casein aggregation. To verify our proposition, we carried out several control experiments with RCM κ-casein (10 and 100 μM) at pH 6.8, 37 °C (Fig. S1e, f and Fig. S2). In the first set of controls, we added 2.5 mM $CaCl_2$ to monomeric κ-casein in the absence of β-casein and monitored the time-dependent changes in κ-casein hydrodynamic diameter. At 10 μM κ-casein, we observed two distinct populations of species with hydrodynamic diameters (D_h) of ~7 and ~22 nm (Fig. S1e) that could be attributed to monomeric and oligomeric RCM κ-casein, respectively. Interestingly, the species with similar D_h ~ 22 nm were also observed upon the addition of calcium ions to a solution containing 1 : 1 molar ratio of β-casein (10 μM) and RCM κ-casein (10 μM) (Fig. 4b). On the other hand, at 100 μM κ-casein, we observed species with primarily D_h ~18 nm (Fig. S1f) that corroborated with results obtained at a 1 : 10 molar ratio of β-casein (10 μM) and RCM κ-casein (100 μM) (Fig. 4f) upon addition of calcium ions. In the second set of controls, we co-incubated β- and κ-caseins at pH

6.8, 37 °C, in the absence of calcium ions, and monitored the changes in hydrodynamic size of the protein mixture as a function of time. Both a 1 : 1 and 1 : 10 mixture of β-casein (D_h ~ 7 nm) and RCM κ-casein (D_h ~ 7–10 nm) indicated the presence of species with D_h ~ 14–18 nm throughout the timescale of our experiment that could be assigned to an inter-protein complex (Fig. S2a and b). Therefore, taken together, we inferred that the addition of Ca^{2+}-ions into a mixture of β-casein and κ-casein plausibly led to the formation of κ-casein oligomers owing to ion condensation on the protein backbone. Additionally, in the presence of RCM κ-casein, β-casein probably exists as monomers and participates in the inter-protein complex formation that impedes the binding of calcium ions to β-casein inhibiting its self-assembly. These observations corroborated our results obtained from the turbidity assays that depicted a dose-dependent reduction in the solution turbidity upon the pre-addition of κ-casein into β-casein solution indicating a reduction in the extent of β-casein aggregation. As mentioned earlier, the plausible formation of a fuzzy coat by the C-terminal region of κ-casein, which acted as a steric and an electrostatic barrier presumably suppressed the aggregation propensity of β-casein.

Next, we investigated the nanoscopic morphologies of the aggregation reaction mixture, in the presence of pre-added RCM κ-casein at varied molar ratios (*viz.* 1 : 1, 1 : 4, and 1 : 10) by TEM imaging (Fig. 4c, e and g). At a 1 : 1 molar ratio of β-casein : κ-casein, we observed a few spherical aggregates (Fig. 4c) whose number as well as size reduced significantly at a 1 : 4 molar ratio (Fig. 4e) indicating the presence of primarily oligomers. At a 1 : 10 molar ratio, we did not observe any protein oligomers/aggregates (Fig. 4g), indicating a complete suppression of β-casein aggregation by RCM κ-casein. Taken together, our turbidity assays, DLS measurements, and TEM imaging validated our hypothesis that monomeric κ-casein acts as a chaperone and effectively inhibits the Ca^{2+}-induced aggregation of β-casein, driven *via* electrostatic screening of the phosphorylated serine residues (CaP-SLiM) of β-casein, that restricted the binding of calcium ions.[56] Consequently, the multivalent interactions between the β-casein chains pivotal for the self-assembly were hindered. Additionally, the predominance of PP-II conformations in both β- and κ-caseins, plausibly promotes the formation of sticky intermolecular contacts between the two polypeptides leading to the formation of an inter-protein complex, and hence, diminishes the propensity towards Ca^{2+}-induced self-assembly. The effectiveness of the inhibitory activity of monomeric RCM κ-casein was also found to be dose-dependent. This is in accordance with the proposed role of κ-casein in stabilizing the casein micelles in milk.[53]

2.6. Dissolution of preformed Ca^{2+}-induced β-casein aggregates by monomeric κ-casein (post-added)

Next, we asked whether the addition of RCM κ-casein to preformed Ca^{2+}-induced β-casein aggregates (post-addition approach) could disintegrate the amorphous aggregates, similar to that

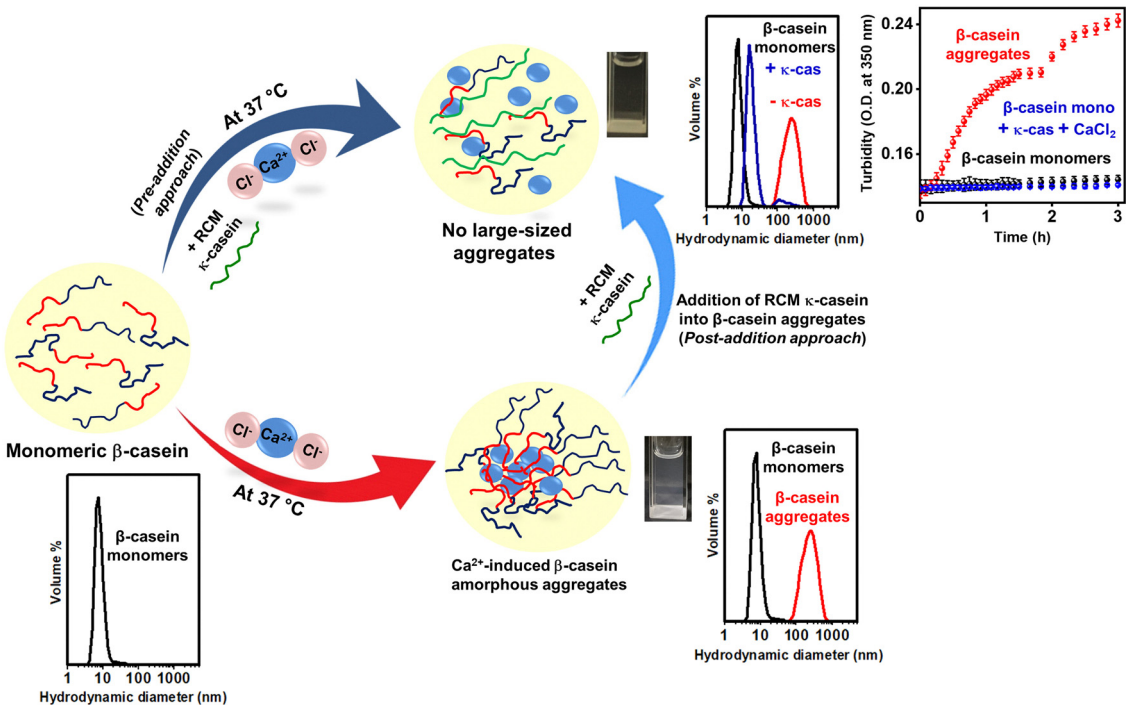

Fig. 5 Schematic representation of Ca^{2+}-induced β-casein aggregation in the absence and presence of reduced and carboxymethylated (RCM) κ-casein under physiological conditions suggesting the chaperonic activity of κ-casein. A two-pronged approach was adopted for the addition of κ-casein; pre-addition approach depicts adding RCM κ-casein at the onset of β-casein aggregation, which prevented the formation of large aggregates. In the post-addition approach, RCM κ-casein was added to the preformed β-casein aggregates, which led to a dissolution of the aggregates into oligomers. The cuvettes shown here are the same as that shown in Fig. 3d (above).

observed with post-addition of NaCl (Fig. 1). For these experiments, we monitored β-casein aggregation in the presence of calcium ions by measuring the changes in the hydrodynamic size of the protein at pH 6.8, and 37 °C (Fig. 4h). After 3 hours, we added monomeric κ-casein to the preformed aggregates and the hydrodynamic size shifted from ∼200 nm to ∼20 nm almost instantaneously (Fig. 4h) depicting the dissolution of aggregates concomitant with the formation of smaller oligomeric species whose size remained almost constant as a function of time. This was further ascertained from the morphological characteristics of the disintegrated β-casein aggregates by utilizing transmission electron microscopy (Fig. 4i, j and Fig. S3a, b) upon the addition of monomeric RCM κ-casein into the pre-formed Ca^{2+}-induced β-casein aggregates. Overall, it was clearly evident that the monomeric κ-casein disrupted the preformed β-casein aggregates effectively under physiological conditions.

3. Conclusions

In summary (Fig. 5), using turbidity assays, the light scattering technique, and electron microscopy, we demonstrated that monomeric κ-casein exhibits its chaperonic activity and inhibits calcium ion-induced β-casein amorphous aggregation under physiological conditions. Based on the charge patterning of both the IDPs, we propose that the inhibitory action is attributed to the electrostatic interactions (*e.g.* between arginine/lysine/histidine–aspartate/glutamate) between β- and κ-caseins, as well as an effective shielding of the phosphorylated serines (CaP-SLiM) of β-casein by κ-casein, that serve as putative binding sites of divalent calcium ions. Impediment of the CaP-SLiM further restricts the binding of calcium ions, which effectively hinders the formation of inter-casein bridges, and multivalent interactions between the β-casein polypeptides required for β-casein self-assembly as evident from the turbidity assays, DLS measurements, and TEM images. Moreover, the presence of P, Q-rich sequences in both β- and κ-caseins, comprising preponderant PP-II secondary structures, presumably facilitates the formation of sticky intermolecular contacts between the polypeptides that further enables the formation of inter-protein complexes and hence, reduces/abolishes the aggregation propensity of β-casein. Additionally, we show for the first time, to the best of our knowledge, that sodium chloride (NaCl) and monomeric κ-casein triggered the dissolution of preformed β-casein amorphous aggregates resulting in off-pathway, soluble oligomers. Since β-casein has potential widespread applications owing to their nutritional and functional values in the food sector and food chaperones are fundamentally recruited in the food matrices, we believe that the findings from this study will have implications in devising strategies for regulating the self-assembly and disassembly processes of β-casein and other food proteins.

4. Materials and methods

To monitor the calcium-induced aggregation of β-casein (pH 6.8, 10 mM imidazole-HCl buffer) in the presence of reduced and carboxymethylated (RCM) κ-casein, the β-casein stock solution was diluted to a final protein concentration of 10 μM. The aggregation was investigated by a two-pronged approach, namely, pre-addition and post-addition of RCM κ-casein. The aggregation kinetics were monitored at 37 °C using turbidity assays and dynamic light scattering. The changes in the nanoscopic morphologies of β-casein aggregates were examined using TEM. For all the experimental and other technical details, please refer to the SI.

Author contributions

M. B. conceived and designed research, J. K. performed research, J. K. and M. B. analyzed the data, and J. K. and M. B. wrote the article.

Conflicts of interest

There are no conflicts of interest to declare.

Data availability

The data supporting this article have been included as part of the supplementary information (SI). Supplementary information: all the experimental and technical details, along with additional figures (DLS and TEM images), are available. See DOI: **https://doi.org/10.1039/d5cp02431e**.

Acknowledgements

J. K. is thankful to the Ministry of Education (MoE) for the fellowship and M. B. acknowledges financial assistance from MoE for the STARS Research Grant (MoE-STARS/STARS-2/2023-0402) and the erstwhile Science and Engineering Research Board (SERB), now ANRF, for the POWER Research Grant (SPG/2021/001574). We are grateful to TIET Patiala for the infrastructural facilities, Prof. Kamaldeep Paul (TIET Patiala) for allowing us to use the plate-reader in his laboratory, and the CD and TEM central facilities at IISER Mohali. We also thank Prof. Samrat Mukhopadhyay (IISER Mohali) for allowing us to use the DLS instrument available in his laboratory and the members of the Bhattacharya lab (TIET Patiala) for reading the manuscript critically.

References

1 G. C. de Andrade, M. F. Mota, D. N. Moreira-Ferreira, J. L. Silva, G. A. P. de Oliveira and M. A. Marques, *Adv. Protein Chem. Struct. Biol.*, 2025, **145**, 145–217.
2 T. S. Chisholm and C. A. Hunter, *Chem. Soc. Rev.*, 2024, **53**, 1354–1374.
3 F. R. Khorsand, F. Aziziyan and K. Khajeh, *Prog. Mol. Biol. Transl. Sci.*, 2024, **206**, 55–83.
4 B. Dabirmanesh, K. Khajeh and V. N. Uversky, *Prog. Mol. Biol. Transl. Sci.*, 2024, **206**, 1–10.

5 N. Louros, J. Schymkowitz and F. Rousseau, *Nat. Rev. Mol. Cell Biol.*, 2023, **24**, 912–933.
6 M. S. Hipp and F. U. Hartl, *J. Mol. Biol.*, 2024, **436**, 168615.
7 M. S. Hipp, P. Kasturi and F. U. Hartl, *Nat. Rev. Mol. Cell Biol.*, 2019, **20**, 421–435.
8 J. M. Storey and K. B. Storey, *Cell Stress Chaperones*, 2023, **28**, 455–466.
9 C. Hu, J. Yang, Z. Qi, H. Wu, B. Wang, F. Zou, H. Mei, J. Liu, W. Wang and Q. Liu, *MedComm*, 2020, **3**, 161.
10 A. M. de Graff, D. E. Mosedale, T. Sharp, K. A. Dill and D. J. Grainger, *PLoS Comput. Biol.*, 2020, **16**, e1008460.
11 A. Akbari, F. Bamdad and J. Wu, *Food Funct.*, 2018, **9**, 3597.
12 Y. H. Yong and E. A. Foegeding, *J. Agric. Food Chem.*, 2010, **58**, 685–693.
13 M. M. Rahman, R. S. Pires, A. Herneke, V. Gowda, M. Langton, H. Biverstal and C. Lendel, *Sci. Rep.*, 2023, **13**, 985.
14 K. J. A. Jansens, M. A. Lambrecht, I. Rombouts, M. M. Morera, K. Brijs, F. Rousseau, J. Schymkowitz and J. A. Delcour, *Compr. Rev. Food Sci. Food Saf.*, 2019, **18**, 1256–1276.
15 X. Fan, Q. Wang, H. Jin, Y. Zhang, Y. Yang, Z. Li, G. Jin and L. Sheng, *Food Chem.*, 2024, **446**, 138881.
16 S. M. Loveday, *Nutr. Res. Rev.*, 2023, **36**, 544–559.
17 J. A. Carver and C. Holt, in *Casein Structural Properties, Uses, Health Benefits and Nutraceutical Applications*, ed. M. El-Bakry and B. M. Mehta, Academic Press, Elsevier, Amsterdam, 2024, ch. 6, pp. 63–91.
18 C. Holt and J. A. Carver, *J. Dairy Sci.*, 2024, **107**, 5259–5279.
19 J. K. Raynes, J. Mata, K. L. Wilde, J. A. Carver, S. M. Kelly and C. Holt, *J. Struct. Biol.: X*, 2024, **9**, 100096.
20 A. Horvath, M. Fuxreiter, M. Vendruscolo, C. Holt and J. A. Carver, *FEBS Lett.*, 2022, **596**, 2072–2085.
21 J. M. L. Heck, C. Olieman, A. Schennink, H. J. F. van Valenberg, M. H. P. W. Visker, R. C. R. Meuldijk and A. C. M. van Hooijdonk, *Int. Dairy J.*, 2008, **18**, 548–555.
22 A. Mora-Gutierrez, T. F. Kumosinski and H. M. Farrell Jr, *J. Dairy Sci.*, 1991, **74**, 3303–3307.
23 H. Mohammad-Beigi, W. Wijaya, M. Madsen, Y. Hayashi, R. Li, T. A. M. Rovers, T. C. Jæger, A. K. Buell, A. B. Hougaard, J. J. K. Kirkensgaard, P. Westh, R. Ipsen and B. Svensson, *Food Hydrocolloids*, 2023, **137**, 108373.
24 C. Holt and J. A. Carver, *Int. Dairy J.*, 2022, **126**, 105292.
25 E. Bahraminejad, D. Paliwal, M. Sunde, C. Holt, J. A. Carver and D. C. Thorn, *Biochim. Biophys. Acta, Proteins Proteomics*, 2022, **1870**, 140854.
26 M. A. Lambrecht, K. J. A. Jansens, I. Rombouts, K. Brijs, F. Rousseau, J. Schymkowitz and J. A. Delcour, *Compr. Rev. Food Sci. Food Saf.*, 2019, **18**, 1277–1291.
27 S. Arya, P. Dogra, N. Jain and S. Mukhopadhyay, *J. Chem. Sci.*, 2017, **129**, 1817–1827.
28 J. Leonil, G. Henry, D. Jouanneau, M.-M. Delage, V. Forge and J.-L. Putaux, *J. Mol. Biol.*, 2008, **381**, 1267–1280.
29 D. C. Thorn, S. Meehan, M. Sunde, A. Rekas, S. L. Gras, C. E. MacPhee, C. M. Dobson, M. R. Wilson and J. A. Carver, *Biochemistry*, 2005, **44**, 17027–17036.
30 H. M. Farrell Jr., P. H. Cooke, E. D. Wickham, E. D. Piotrowski and P. T. Hoagland, *J. Protein Chem.*, 2003, **22**, 259–273.
31 Y. Luo, K. Pan and Q. Zhong, *Int. J. Pharm.*, 2015, **486**, 59–68.
32 A. Zhang, H. Xie, N. Liu, B.-L. Chen, H. Ping, Z.-Y. Fu and B.-L. Su, *RSC Adv.*, 2016, **6**, 110362–110366.
33 S. Wang, T. Langrish and M. Leszczynski, *Drying Technol.*, 2010, **28**, 422–429.
34 J. A. Carver, H. Ecroyd, R. J. W. Truscott, D. C. Thorn and C. Holt, *Acc. Chem. Res.*, 2018, **51**, 745–752.
35 H. M. Sanders, B. Jovcevski, J. A. Carver and T. L. Pukala, *Biochem. J.*, 2020, **477**, 629–643.
36 T. M. Treweek, in *Milk Protein*, ed. W. L. Hurley, InTech, Rijeka, Croatia, 2012, pp. 85–119.
37 P. E. Morgan, T. M. Treweek, R. A. Lindner, W. E. Price and J. A. Carver, *J. Agric. Food Chem.*, 2005, **53**, 2670–2683.
38 X. Zhang, X. Fu, H. Zhang, C. Liu, W. Jiao and Z. Chang, *Int. J. Biochem. Cell Biol.*, 2005, **37**, 1232–1240.
39 A. Runthala, M. Mbye, M. Ayyash, Y. Xu and A. Kamal-Eldin, *Molecules*, 2023, **28**, 1–36.
40 J. Bhattacharya and K. P. Das, *J. Biol. Chem.*, 1999, **274**, 15505–15509.
41 H. Ecroyd, D. C. Thorn, Y. Liu and J. A. Carver, *Biochem. J.*, 2010, **429**, 251–260.
42 R. Yousefi and S. Jalili, *Colloids Surf., B*, 2011, **88**, 497–504.
43 M. Li, M. A. E. Auty, S. V. Crowley, A. L. Kelly, J. A. O'Mahony and A. Brodkorb, *Food Hydrocolloids*, 2019, **88**, 190–198.
44 J. Kaur and M. Bhattacharya, *J. Colloid Interface Sci.*, 2025, **697**, 137916.
45 M. Mussel, P. J. Basser and F. Horkay, *Soft Matter*, 2019, **15**, 4153–4161.
46 H. K. Ju, S.-J. Hwang, C.-J. Jeon, G.-M. Lee and S. K. Yoon, *J. Biotechnol.*, 2009, **143**, 145–150.
47 D. Singla and M. Bhattacharya, *J. Phys. Chem. B*, 2022, **126**, 8760–8770.
48 C. Holt, J. A. Carver, H. Ecroyd and D. C. Thorn, *J. Dairy Sci.*, 2013, **96**, 6127–6146.
49 A. S. Holehouse, R. K. Das, J. N. Ahad, M. O. G. Richardson and R. V. Pappu, *Biophys. J.*, 2017, **112**, 16–21.
50 A. H. Mao, S. L. Crick, A. Vitalis, C. L. Chicoine and R. V. Pappu, *Proc. Natl. Acad. Sci. U. S. A.*, 2010, **107**, 8183–8188.
51 N. Jain, M. Bhattacharya and S. Mukhopadhyay, *Biophys. J.*, 2011, **101**, 1720–1729.
52 B. T. O'Kennedy and J. S. Mounsey, *J. Agric. Food Chem.*, 2006, **54**, 5637–5642.
53 L. K. Creamer, J. E. Plowman, M. J. Liddell, M. H. Smith and J. P. Hill, *J. Dairy Sci.*, 1998, **81**, 3004–3012.
54 D. J. McMahon and R. J. Brown, *J. Dairy Sci.*, 1983, **67**, 499–512.
55 S. Dauphas, N. Mouhous-Riou, B. Metro, A. R. Mackie, P. J. Wilde, M. Anton and A. Riaublanc, *Food Hydrocolloids*, 2005, **19**, 387–393.
56 F. Guyomarc'h, M. Nono, T. Nicolai and D. Durand, *Food Hydrocolloids*, 2009, **23**, 1103–1110.